JOURNAL OF GUIDANCE, CONTROL, AND DYNAMICS
Vol. 31, No. 4, July–August 2008

High-Performance Spacecraft Adaptive Attitude-Tracking Control Through Attracting-Manifold Design

Dongeun Seo* and Maruthi R. Akella†
University of Texas at Austin, Austin, Texas 78712

DOI: 10.2514/1.33308

Virtually every existing adaptive attitude control solution is based on the certainty-equivalence principle, which permits the adaptive controller structure to be based upon the deterministic feedback control algorithm (controller design based on nominal system information without any inertia-parameter uncertainty) and to be used in conjunction with a suitable adaptive parameter-estimation algorithm. However, one of the main drawbacks of the certainty-equivalence-based adaptive control methodology is the arbitrary degradation in closed-loop performance due to the adaptation (parameter-estimation) process, which acts like a forcing disturbance (uncertain parameter effect) imposed onto the deterministic closed-loop control dynamics. In this paper, we significantly deviate from the classical certainty-equivalence-based adaptive control framework and develop, for the first time (to our best knowledge), a noncertainty-equivalent adaptive attitude control algorithm. This novel control design process eliminates the deleterious performance-degradation effects of the certainty-equivalence controller through the introduction of a stable attracting manifold into the adaptation process, such that the resulting closed-loop adaptive attitude control dynamics recover the deterministic (ideal) case of closed-loop attitude controller performance (i.e., no uncertain parameter effects). In addition to detailed derivations of the new controller design and a rigorous sketch of all the associated stability and attitude error convergence proofs, we present numerical simulation results that not only illustrate the various features of the new noncertainty-equivalent controller design methodology but also highlight the ensuing closed-loop-performance benefits when compared with the conventional certainty-equivalence-based adaptive control schemes.

I. Introduction

THE nonlinear control problem associated with spacecraft attitude dynamics has been extensively studied and various proportional–derivative types of stabilizing feedback solutions are currently available in the literature [1–4]. In particular, the application of model-reference adaptive control theory for stabilizing spacecraft-attitude-tracking dynamics in the presence of arbitrarily large inertia matrix uncertainties has been largely enabled by the crucial fact that the governing dynamics permit affine representation of inertia-related terms [5–7]. Nearly every one of these existing adaptive attitude-tracking control solutions is based upon the classical certainty-equivalence (CE) principle [8,9], which permits the adaptive controller to retain a structure that is identical to that of the deterministic-case controller wherein the inertia parameters are fully available (no uncertainty), except for the introduction of an additional carefully designed parameter-update (estimation) mechanism that ensures stability with the adaptive controller and boundedness of all resulting closed-loop signals.

In theoretical terms, the closed-loop error dynamics generated by CE-based adaptive control solutions are exactly equivalent to the deterministic-case control error dynamics whenever the estimated parameters coincide with their corresponding unknown true values. Of course, this happens only when the underlying reference trajectory satisfies suitable persistence of excitation (PE) conditions [8]. As a result, typically, the control performance of CE-based adaptive attitude control methods for either setpoint regulation or trajectory-tracking problems can, at best, match the performance of the deterministic-case controller, but only when the PE hypothesis ensures sufficiently fast convergence of parameter estimates to their true values. However, in practice, the closed-loop performance obtained from CE-based adaptive controllers is often seen to be arbitrarily poor when compared with the ideal deterministic control case, due to nonsatisfaction of PE conditions and/or slow convergence rates for the parameter estimates. All of these factors ultimately result in imposing wasteful rotational motion, due to the control action, and therefore significant increases within the torque requirements and fuel costs.

This aforementioned performance degradation of CE-based adaptive control in attitude-tracking/regulating problems is mainly caused by the fact that search/estimation efforts of the parameter-update law act like an additive disturbance imposed onto the deterministic-case closed-loop dynamics. Another potential cause of performance degradation is the fact that parameter-estimation dynamics are driven by the state-regulation errors or tracking errors, which results in the undesirable feature of parameter estimates being unable to get locked onto their corresponding true values, even if (at any given instant during the estimation process) the estimates are equal to their true values. Moreover, parameter estimates from CE-based adaptive control methods always deviate (drift) from their corresponding true values, even if they are initiated to exactly coincide with their true values whenever nonzero tracking/regulating error exists. Therefore, one may think of improving the overall closed-loop performance of adaptive control schemes by either eliminating (in a stable fashion) the disturbance type of terms within closed-loop error dynamics arising due to estimation of uncertain parameters or by forcing the parameter estimates to stay locked at their true parameters once they are attained during the estimation process. A technical challenge in this matter is to design such a parameter-update rule that would deal with both uncertain parameter effects and estimation drift.

The main contribution of this paper is the introduction of a new noncertainty-equivalence (non-CE) adaptive attitude-tracking control method that has potential to deliver significantly superior closed-loop performance when compared with the classical CE-based adaptive control schemes. Our results are partly motivated by the recently formulated immersion and invariance (I–I) adaptive

Received 6 July 2007; revision received 15 November 2007; accepted for publication 20 November 2007.

*Graduate Research Assistant, Ph.D. Candidate, Department of Aerospace Engineering and Engineering Mechanics; seode@mail.utexas.edu.

†Associate Professor, Department of Aerospace Engineering and Engineering Mechanics; makella@mail.utexas.edu. Associate Fellow AIAA.

control theory [10–12]. The I–I design is essentially a non-CE-based adaptive control methodology that overcomes many of the performance limitations arising from CE-based designs. However, applications of I–I adaptive control to general multi-input nonlinear systems have thus far been somewhat limited because of certain restrictive "realizability" and "manifold attractivity" conditions [10]. Specifically, in the adaptive spacecraft-attitude-tracking control problem with three independent control torques, it is currently not possible to design an I–I adaptive tracking controller while satisfying the realizability and manifold attractivity conditions [10]. In this paper, we extend the I–I framework by circumventing the restrictions implicit within the I–I adaptive control design scheme. We are able to do so while preserving all the key beneficial features of the I–I adaptive control methodology by introducing a stable linear filter for the regressor matrix so that the parameter-adaptation dynamics reside within a stable and attracting manifold. In particular, our novel controller design approach ensures that the additive disturbance type of term arising within the closed-loop dynamics due to the parameter-estimation error decays to zero, independent of the satisfaction of any additional PE-type conditions. Moreover, the rate of this decay can be prescribed by the designer to be arbitrarily fast. Yet another interesting and important consequence of our new result that is never possible with existing CE-based solutions is the fact that the proposed adaptive parameter-estimation process automatically stops if and when the parameter estimates happen to coincide with their corresponding unknown true values. Our formulation is given in terms of the globally valid (singularity-free) four-dimensional unit-quaternion representation for attitude. Assuming the spacecraft inertia matrix to be unknown, we make use of full state feedback (i.e., perfect measurement of the body angular rate and the attitude measurement in terms of the quaternion parameterization to guarantee *globally stable* closed-loop behavior with asymptotic convergence of regulation/tracking errors for all possible initial conditions). It is pertinent here to observe the fact that the set of special group of rotation matrices that describe body orientation in three dimensions $SO(3)$ is not a contractible space, and hence quaternion-based formulations do not permit globally continuous stabilizing controllers [1,2]. In this sense, we adopt the standard terminology/notion of (almost) global stability for this problem to imply stability over an open and dense set in $SO(3)$, as is usually seen in literature dealing with this problem [13]. It should also be emphasized that the basic approach outlined in this paper can be readily extended to other attitude representations, including minimal three-parameter sets [14–16].

The paper is organized as follows. In Sec. II, the attitude-tracking control problem is formulated, starting from a basic description of quaternion kinematics and the Euler rotational-dynamics equations. In Sec. III, the main theoretical results of this paper are presented, along with detailed stability proofs. In Sec. IV, we show numerical simulation results for spacecraft-attitude-tracking control problems, comparing our new non-CE method with a conventional CE-based method to highlight the performance improvement due to the presence of an attracting manifold within the proposed parameter-adaptation mechanism. We conclude the paper with Sec. V by drawing appropriate concluding remarks.

II. Problem Formulation

Euler's rotational equations of motion state the rigid-body attitude dynamics in terms of its angular velocity $\boldsymbol{\omega}(t) \in \mathbb{R}^3$ prescribed in a body-fixed frame, the mass moment of inertia defined through the 3×3 symmetric positive-definite matrix J (assumed to be an unknown constant in this paper), and an external control torque $\boldsymbol{u}(t) \in \mathbb{R}^3$, as follows:

$$J\dot{\boldsymbol{\omega}}(t) = -S(\boldsymbol{\omega}(t))J\boldsymbol{\omega}(t) + \boldsymbol{u}(t) \tag{1}$$

where the skew-symmetric matrix operator $S(\cdot)$ represents the vector cross-product operation between any two vectors, as defined by $S(\boldsymbol{x})\boldsymbol{y} = \boldsymbol{x} \times \boldsymbol{y}$ for any $\boldsymbol{x}, \boldsymbol{y} \in \mathbb{R}^3$. The corresponding kinematic differential equations governing the attitude motion are given by

$$\dot{\boldsymbol{q}}(t) = \tfrac{1}{2}E(\boldsymbol{q}(t))\boldsymbol{\omega}(t); \qquad E(\boldsymbol{q}) = \Big[-\boldsymbol{q}_v^T q_o I_{3\times3} + S(\boldsymbol{q}_v)\Big]^T \tag{2}$$

where $\boldsymbol{q}(t)$ is the four-dimensional unit-norm constrained quaternion vector representing the attitude of the body-fixed frame $\mathcal{F}_B$ with respect to the inertial frame $\mathcal{F}_I$, and $I_{3\times3}$ is the 3×3 identity matrix. In the following development, for the sake of notational simplicity, the time argument t is left out, except when it is noted for emphasis. We denote q_o and $\boldsymbol{q}_v$ as scalar and vector parts of the unit quaternion, respectively (i.e., $\boldsymbol{q} = [q_o, \boldsymbol{q}_v]^T$, along with the unit-quaternion constraint $\boldsymbol{q}^T\boldsymbol{q} = 1$). The direction cosine matrix can be obtained from the quaternion vector through the following identity [3]:

$$C(\boldsymbol{q}) = I_{3\times3} - 2q_o S(\boldsymbol{q}_v) + 2S^2(\boldsymbol{q}_v) \tag{3}$$

Because it is natural for the commanded angular velocity to be specified in its own reference frame $\mathcal{F}_C$, we assume the commanded bounded angular velocity $\boldsymbol{\omega}_C$ to be stated in the reference frame $\mathcal{F}_C$ and we denote $\boldsymbol{q}_C$ to orient the commanded reference frame $\mathcal{F}_C$ with respect to the inertial frame $\mathcal{F}_I$. Then the attitude and angular-velocity tracking errors are obtained as follows:

$$C(\delta\boldsymbol{q}) = C(\boldsymbol{q})C^T(\boldsymbol{q}_C); \qquad \delta\boldsymbol{\omega} = \boldsymbol{\omega} - C(\delta\boldsymbol{q})\boldsymbol{\omega}_C \tag{4}$$

where the attitude error quaternion $\delta\boldsymbol{q} = [\delta q_o, \delta\boldsymbol{q}_v]^T$ follows our notational convention. We note here that $\mathcal{F}_B \to \mathcal{F}_C$ means $C(\delta\boldsymbol{q}) \to I_{3\times3}$ (i.e., $\delta\boldsymbol{q} \to [\pm1, 0, 0, 0]^T$). The overall attitude-tracking error dynamics are obtained by differentiating Eq. (4) with respect to time, as follows [1,3,6,7]:

$$\delta\dot{\boldsymbol{q}} = \tfrac{1}{2}E(\delta\boldsymbol{q})\delta\boldsymbol{\omega} \tag{5}$$

$$J\delta\dot{\boldsymbol{\omega}} = -S(\boldsymbol{\omega})J\boldsymbol{\omega} + \boldsymbol{u} + J[S(\delta\boldsymbol{\omega})C(\delta\boldsymbol{q})\boldsymbol{\omega}_C - C(\delta\boldsymbol{q})\dot{\boldsymbol{\omega}}_C] \tag{6}$$

wherein the inertia matrix J is unknown and the adaptive control objective is to determine control torque $\boldsymbol{u}(t)$ while employing full-state feedback $[\boldsymbol{\omega}(t), \boldsymbol{q}(t)]$, to achieve boundedness of all closed-loop signals and convergence of tracking errors

$$\lim_{t\to\infty}[\delta\boldsymbol{q}_v(t), \delta\boldsymbol{\omega}(t)] = 0$$

for all possible reference trajectories $[\boldsymbol{\omega}_C(t), \boldsymbol{q}_C(t)]$ and initial conditions $[\boldsymbol{\omega}(0), \boldsymbol{q}(0)]$.

III. Non-CE High-Performance Adaptive Attitude-Tracking Control

In this section, we present a novel non-CE adaptive control method for the attitude-tracking problem represented by Eqs. (5) and (6), and we specifically focus on obtaining closed-loop-performance improvement. The following theorem represents the main results of our paper.

Theorem 1. Consider the attitude-tracking error system equations (5) and (6) with the inertia matrix J being unknown, and suppose that the adaptive control input $\boldsymbol{u}$ is determined through

$$\boldsymbol{u} = -W(\hat{\boldsymbol{\theta}} + \beta) - \gamma W_f W_f^T[k_p(\boldsymbol{\omega}_f - \delta\boldsymbol{q}_v) - \delta\boldsymbol{\omega}] \tag{7}$$

$$\dot{\hat{\boldsymbol{\theta}}} = \gamma W_f^T[(\alpha + k_v)\boldsymbol{\omega}_f + k_p\delta\boldsymbol{q}_v] - \gamma W^T\boldsymbol{\omega}_f \tag{8}$$

$$\beta = \gamma W_f^T\boldsymbol{\omega}_f \tag{9}$$

wherein $k_p, k_v, \gamma > 0$ are any scalar constants, $\alpha = k_p + k_v$, and the regressor matrix W is constructed in the following fashion:

$$\begin{aligned} W\boldsymbol{\theta}^* = {} & -S(\boldsymbol{\omega})J\boldsymbol{\omega} + J[S(\delta\boldsymbol{\omega})C(\delta\boldsymbol{q})\boldsymbol{\omega}_C - C(\delta\boldsymbol{q})\dot{\boldsymbol{\omega}}_C] \\ & + J(k_v\delta\boldsymbol{\omega} + k_p\delta\dot{\boldsymbol{q}}_v + \alpha k_p\delta\boldsymbol{q}_v) \end{aligned} \tag{10}$$

where $\boldsymbol{\theta}^* = [J_{11}, J_{12}, J_{13}, J_{22}, J_{23}, J_{33}]^T$ represents the elements of

the unknown symmetric inertia matrix $J = [J_{ij}]$. Further, the signals W_f and $\boldsymbol{\omega}_f$ required when computing the control input $\boldsymbol{u}$ in Eq. (7) are obtained from stable first-order linear filter dynamics:

$$\dot{\boldsymbol{\omega}}_f = -\alpha\boldsymbol{\omega}_f + \delta\boldsymbol{\omega} \tag{11}$$

$$\dot{W}_f = -\alpha W_f + W \tag{12}$$

with arbitrary initial conditions $W_f(0) \in \mathbb{R}^{3\times 6}$ and $\boldsymbol{\omega}_f(0) \in \mathbb{R}^3$. Then, for all possible initial conditions $[\boldsymbol{\omega}(0), \boldsymbol{q}(0)]$ and reference trajectories $[\boldsymbol{\omega}_C(t), \boldsymbol{q}_C(t)]$, the closed-loop is globally asymptotically stable, leading to the convergence condition

$$\lim_{t\to\infty}[\delta\boldsymbol{q}_v(t), \delta\boldsymbol{\omega}(t)] = 0$$

Proof. First, we rearrange Eq. (6) into parameter-affine form, consistent with the definition of the regressor matrix W in Eq. (10). Starting with the addition and subtraction of terms

$$J(k_v\delta\boldsymbol{\omega} + k_p\delta\dot{\boldsymbol{q}}_v + \alpha k_p\delta\boldsymbol{q}_v)$$

to the right-hand side of Eq. (6) and following up through the regressor definition in Eq. (10) and some minor algebraic manipulations, it is easy to obtain

$$\delta\dot{\boldsymbol{\omega}} = -k_v\delta\boldsymbol{\omega} - k_p(\delta\dot{\boldsymbol{q}}_v + \alpha\delta\boldsymbol{q}_v) + J^{-1}(W\boldsymbol{\theta}^* + \boldsymbol{u}) \tag{13}$$

where k_v and k_p are any scalar positive gains, and $\alpha = k_v + k_p$, as defined earlier in this section. Obviously, the angular-rate-tracking error dynamics in Eq. (6) are algebraically equivalent to Eq. (13); accordingly, we shall henceforth refer the overall attitude-tracking error dynamics to be represented by Eqs. (5) and (13).

Next, we consider (only for purposes of the ensuing stability analysis) a linear filter involving the control signal defined by

$$\dot{\boldsymbol{u}}_f = -\alpha\boldsymbol{u}_f + \boldsymbol{u} \tag{14}$$

so that we are able to work toward introducing a stable and attracting manifold into the adaptation algorithm. Now we transform the attitude-tracking error dynamics into the filtered attitude-tracking error dynamics using Eqs. (11–14). Differentiating both sides of the filter dynamics in Eq. (11) followed by substitution of the angular-velocity error-dynamics equation (13) and the use of Eqs. (11) and (12), we have

$$\begin{aligned}\ddot{\boldsymbol{\omega}}_f &= -\alpha\dot{\boldsymbol{\omega}}_f - k_v\delta\boldsymbol{\omega} - k_p(\delta\dot{\boldsymbol{q}}_v + \alpha\delta\boldsymbol{q}_v) + J^{-1}(W\boldsymbol{\theta}^* + \boldsymbol{u})\\ &= -\alpha\dot{\boldsymbol{\omega}}_f - k_v(\dot{\boldsymbol{\omega}}_f + \alpha\boldsymbol{\omega}_f) - k_p(\delta\dot{\boldsymbol{q}}_v + \alpha\delta\boldsymbol{q}_v)\\ &\quad + J^{-1}[(\dot{W}_f + \alpha W_f)\boldsymbol{\theta}^* + (\dot{\boldsymbol{u}}_f + \alpha\boldsymbol{u}_f)]\end{aligned} \tag{15}$$

Rearrangement of terms in Eq. (15) leads us to the following perfect differential:

$$\begin{aligned}&\frac{\mathrm{d}}{\mathrm{d}t}[\dot{\boldsymbol{\omega}}_f + k_v\boldsymbol{\omega}_f + k_p\delta\boldsymbol{q}_v - J^{-1}(W_f\boldsymbol{\theta}^* + \boldsymbol{u}_f)]\\ &\quad = -\alpha[\dot{\boldsymbol{\omega}}_f + k_v\boldsymbol{\omega}_f + k_p\delta\boldsymbol{q}_v - J^{-1}(W_f\boldsymbol{\theta}^* + \boldsymbol{u}_f)]\end{aligned} \tag{16}$$

for which the solution may be immediately established by

$$\dot{\boldsymbol{\omega}}_f = -k_v\boldsymbol{\omega}_f - k_p\delta\boldsymbol{q}_v + J^{-1}(W_f\boldsymbol{\theta}^* + \boldsymbol{u}_f) + \varepsilon e^{-\alpha t} \tag{17}$$

where the exponentially decaying term $\boldsymbol{\eta}(t) \doteq \varepsilon e^{-\alpha t}$ on the right-hand side of the preceding equation is characterized by

$$\begin{gathered}\dot{\boldsymbol{\eta}} = -\alpha\boldsymbol{\eta}\\ \boldsymbol{\eta}(0) = \varepsilon = [\dot{\boldsymbol{\omega}}_f(0) + k_v\delta\boldsymbol{q}_v(0) - J^{-1}(W_f(0)\boldsymbol{\theta}^* + \boldsymbol{u}_f(0))]\end{gathered} \tag{18}$$

We now suppose the filtered control signal $\boldsymbol{u}_f$ be specified as follows:

$$\boldsymbol{u}_f = -W_f(\hat{\boldsymbol{\theta}} + \boldsymbol{\beta}) \tag{19}$$

in such a way that the composite term $\hat{\boldsymbol{\theta}} + \boldsymbol{\beta}$ indicates an instantaneous estimate for the unknown parameter vector $\boldsymbol{\theta}^*$, which therefore amounts to a significant departure from the classical certainty-equivalence adaptive control methodology. Accordingly, Eq. (17) becomes

$$\dot{\boldsymbol{\omega}}_f = -k_v\boldsymbol{\omega}_f - k_p\delta\boldsymbol{q}_v - J^{-1}W_f\boldsymbol{z} + \varepsilon e^{-\alpha t} \tag{20}$$

wherein the quantity $\boldsymbol{z} \doteq \hat{\boldsymbol{\theta}} + \boldsymbol{\beta} - \boldsymbol{\theta}^*$ is introduced to indicate the parameter-estimation error. The dynamics of the parameter-estimation error can be derived by making use of Eqs. (8), (9), and (20) to yield the following:

$$\dot{\boldsymbol{z}} = \dot{\hat{\boldsymbol{\theta}}} + \dot{\boldsymbol{\beta}} = -\gamma W_f^T J^{-1} W_f\boldsymbol{z} + \gamma W_f^T\boldsymbol{\eta} \tag{21}$$

Now consider the lower-bounded Lyapunov-like function given by

$$V = \frac{1}{2}\boldsymbol{\omega}_f^T\boldsymbol{\omega}_f + (\delta q_o - 1)^2 + \delta\boldsymbol{q}_v^T\delta\boldsymbol{q}_v + \frac{\zeta}{2\lambda_{\min}}\boldsymbol{z}^T\boldsymbol{z} + \frac{\mu}{2}\boldsymbol{\eta}^T\boldsymbol{\eta} \tag{22}$$

where $\lambda_{\min}$ is the minimum eigenvalue of the unknown symmetric positive-definite inertia matrix J, $\max[1/kv, 1/kp]\cdot 9/(4\gamma)$, and $\max[1/kv, 1/kp]\cdot 9/(4\alpha)$. By taking the time derivative of V along trajectories generated from Eqs. (5), (8), (9), (18), and (20), we have the following:

$$\begin{aligned}\dot{V} &= \boldsymbol{\omega}_f^T\dot{\boldsymbol{\omega}}_f - (\delta q_o - 1)\delta\boldsymbol{q}_v^T\delta\boldsymbol{\omega} + \delta\boldsymbol{\omega}\\ &\quad + \delta\boldsymbol{q}_v^T[\delta q_o\delta\boldsymbol{\omega} + S(\delta\boldsymbol{q}_v)\delta\boldsymbol{\omega}] + \frac{\zeta}{\lambda_{\min}}\boldsymbol{z}^T\dot{\boldsymbol{z}} + \mu\boldsymbol{\eta}^T\dot{\boldsymbol{\eta}}\\ &= \boldsymbol{\omega}_f^T(-k_v\boldsymbol{\omega}_f - k_p\delta\boldsymbol{q}_v - J^{-1}W_f\boldsymbol{z} + \boldsymbol{\eta})\\ &\quad + \delta\boldsymbol{q}_v^T\delta\boldsymbol{\omega} + \frac{\zeta}{\lambda_{\min}}\boldsymbol{z}^T(\dot{\hat{\boldsymbol{\theta}}} + \dot{\boldsymbol{\beta}}) - \mu\alpha\boldsymbol{\eta}^T\boldsymbol{\eta}\\ &= -k_v\|\boldsymbol{\omega}_f\|^2 - k_p\boldsymbol{\omega}_f^T\delta\boldsymbol{q}_v - \boldsymbol{\omega}_f^T J^{-1}W_f\boldsymbol{z} + \boldsymbol{\omega}_f^T\boldsymbol{\eta}\\ &\quad + \delta\boldsymbol{q}_v^T(\dot{\boldsymbol{\omega}}_f + \alpha\boldsymbol{\omega}_f) - \frac{\zeta\gamma}{\lambda_{\min}}\boldsymbol{z}^T W_f^T J^{-1}W_f\boldsymbol{z} - \mu\alpha\boldsymbol{\eta}^T\boldsymbol{\eta}\\ &= -k_v\|\boldsymbol{\omega}_f\|^2 - k_p\boldsymbol{\omega}_f^T\delta\boldsymbol{q}_v - \boldsymbol{\omega}_f^T J^{-1}W_f\boldsymbol{z} + \boldsymbol{\omega}_f^T\boldsymbol{\eta}\\ &\quad + \delta\boldsymbol{q}_v^T(-k_v\boldsymbol{\omega}_f - k_p\delta\boldsymbol{q}_v - J^{-1}W_f\boldsymbol{z} + \boldsymbol{\eta} + \alpha\boldsymbol{\omega}_f)\\ &\quad - \frac{\zeta\gamma}{\lambda_{\min}}\boldsymbol{z}^T W_f^T J^{-1}W_f\boldsymbol{z} - \mu\alpha\boldsymbol{\eta}^T\boldsymbol{\eta}\\ &= -k_v\|\boldsymbol{\omega}_f\|^2 - k_p\|\delta\boldsymbol{q}_v\|^2 - \boldsymbol{\omega}_f^T J^{-1}W_f\boldsymbol{z} + \boldsymbol{\omega}_f^T\boldsymbol{\eta}\\ &\quad - \delta\boldsymbol{q}_v^T J^{-1}W_f\boldsymbol{z} + \delta\boldsymbol{q}_v^T\boldsymbol{\eta} - \frac{\zeta\gamma}{\lambda_{\min}}\boldsymbol{z}^T W_f^T J^{-1}W_f\boldsymbol{z} - \mu\alpha\boldsymbol{\eta}^T\boldsymbol{\eta}\\ &\le -\frac{k_v}{3}\|\boldsymbol{\omega}_f\|^2 - \frac{k_p}{3}\|\delta\boldsymbol{q}_v\|^2 - \frac{\zeta\gamma}{3}\|J^{-1}W_f\boldsymbol{z}\|^2 - \frac{\mu\alpha}{3}\|\boldsymbol{\eta}\|^2\\ &\quad - \frac{k_v}{3}\left(\|\boldsymbol{\omega}_f\|^2 + \frac{3}{k_v}\boldsymbol{\omega}_f^T J^{-1}W_f\boldsymbol{z} + \frac{\zeta\gamma}{k_v}\|J^{-1}W_f\boldsymbol{z}\|^2\right)\\ &\quad - \frac{k_v}{3}\left(\|\boldsymbol{\omega}_f\|^2 - \frac{3}{k_v}\boldsymbol{\omega}_f^T\boldsymbol{\eta} + \frac{\mu\alpha}{k_v}\|\boldsymbol{\eta}\|^2\right)\\ &\quad - \frac{k_p}{3}\left(\|\delta\boldsymbol{q}_v\|^2 + \frac{3}{k_p}\delta\boldsymbol{q}_v^T J^{-1}W_f\boldsymbol{z} + \frac{\zeta\gamma}{k_p}\|J^{-1}W_f\boldsymbol{z}\|^2\right)\\ &\quad - \frac{k_p}{3}\left(\|\delta\boldsymbol{q}_v\|^2 - \frac{3}{k_p}\delta\boldsymbol{q}_v^T\boldsymbol{\eta} + \frac{\mu\alpha}{k_p}\|\boldsymbol{\eta}\|^2\right)\\ &\le -\frac{k_v}{3}\|\boldsymbol{\omega}_f\|^2 - \frac{k_p}{3}\|\delta\boldsymbol{q}_v\|^2 - \frac{\zeta\gamma}{3}\|J^{-1}W_f\boldsymbol{z}\|^2 - \frac{\mu\alpha}{3}\|\boldsymbol{\eta}\|^2\end{aligned} \tag{23}$$

which is negative-semidefinite, indicating boundedness for all closed-loop signals. Further, because V is lower-bounded and monotonic by the negative-semidefiniteness of $\dot{V}$, we know that

$$\int_0^\infty \dot{V}(t)\,\mathrm{d}t$$

exists and is finite, which in turn implies $\boldsymbol{\omega}_f$, $\delta\boldsymbol{q}_v$, $J^{-1}W_f\boldsymbol{z}$, and $\boldsymbol{\eta} \in \mathcal{L}_2 \cap \mathcal{L}_\infty$. This also implies boundedness of $\dot{\boldsymbol{\omega}}_f$, $\delta\dot{\boldsymbol{q}}_v$, $\dot{W}_f$, and $\dot{\boldsymbol{z}}$

from Eqs. (5), (8), (9), (12), and (20). By using Barbalat's lemma, we can now guarantee that

$$\lim_{t\to\infty}[\boldsymbol{\omega}_f(t), \delta\boldsymbol{q_v}(t), J^{-1}W_f(t)\boldsymbol{z}(t)] = 0$$

Based on the last result, we may also show that $\lim_{t\to\infty}\dot{\boldsymbol{\omega}}_f(t) = 0$ from Eq. (20). Finally, from Eq. (11), it follows that $\lim_{t\to\infty}\delta\boldsymbol{\omega}(t) = 0$.

One last step remains now, which is to recover the actual control input $\boldsymbol{u}$ from the filtered control signal $\boldsymbol{u}_f$ defined through Eqs. (14) and (19). This can be accomplished through

$$\boldsymbol{u} = \dot{\boldsymbol{u}}_f + \alpha\boldsymbol{u}_f = -\dot{W}_f(\dot{\hat{\boldsymbol{\theta}}} + \dot{\boldsymbol{\beta}}) + \alpha\boldsymbol{u}_f \tag{24}$$

By substituting Eqs. (8), (9), and (12) into the preceding expression, the adaptive control torque $\boldsymbol{u}$ can be recovered to be the expression given in Eq. (7), thereby completing the Proof of Theorem 1. □

The following observations are now in order:

1) From the positive-definiteness of matrix J and the fact that we are able to prove convergence condition

$$\lim_{t\to\infty} J^{-1}W_f(t)\boldsymbol{z}(t) = 0$$

it follows that the proposed adaptive controller provides for the establishment of an attracting manifold $\mathcal{S}$ defined by

$$\mathcal{S} = \{\boldsymbol{z} \in \mathbb{R}^6 | W_f\boldsymbol{z} = 0\} \tag{25}$$

in such a way that all closed-loop trajectories ultimately end up inside $\mathcal{S}$. Moreover, convergence to this attracting manifold can be made arbitrarily fast by tuning the learning-rate parameter γ present within the control law in Eq. (7). This is a most significant feature of the non-CE adaptive controller derived in this paper, given the fact that the term $J^{-1}W_f(t)\boldsymbol{z}(t)$ essentially arises in Eq. (20) due to the mismatch between the current estimate of the parameter $\hat{\boldsymbol{\theta}} + \boldsymbol{\beta}$ and its corresponding true value $\boldsymbol{\theta}^*$ and therefore plays the role of being an additive disturbance imposed onto the ideal-case (no parameter uncertainty) closed-loop system having dynamics given by

$$\dot{\boldsymbol{\omega}}_f = -k_v\boldsymbol{\omega}_f - k_p\delta\boldsymbol{q_v} + \varepsilon e^{-\alpha t} \tag{26}$$

A primary implication of this assertion is that the closed-loop performance obtained in the ideal case is recovered through the presence of the attracting manifold in the adaptive case: a feature that is seldom available with existing CE-based adaptive control schemes. This statement can be further elaborated based on the fact that conventional CE-based adaptive controllers rely upon the cancellation of the uncertain parameter effects (within the time derivatives of suitable Lyapunov-like candidate functions to render them negative-semidefinite); accordingly, the recovery of the ideal-case (no uncertainty and deterministic control) closed-loop performance happens only after either the parameter estimates converge to their corresponding true values and/or the tracking/regulating errors converge to zero. The role played by the learning-rate parameter γ will be further illuminated in the Numerical Simulations section.

2) The key steps that permit extension of the non-CE-based I–I adaptive control framework [10,11] to the adaptive attitude-tracking control problem for spacecraft are represented through our introduction of the regressor filter in Eq. (12) and the algebraic developments leading to the establishment of Eq. (13), which were made possible by judiciously adding and subtracting the term

$$J(k_v\delta\boldsymbol{\omega} + k_p\delta\dot{\boldsymbol{q}}_{\boldsymbol{v}} + \alpha k_p\delta\boldsymbol{q_v})$$

in the right-hand side of Eq. (6). Also important to note is the fact that only the angular-rate error signal $\delta\boldsymbol{\omega}$ needs to be filtered through Eq. (11) to obtain the signal $\boldsymbol{\omega}_f$ that is required for the controller implementation, whereas no filtering is needed on the attitude error signal represented by the unit-norm constrained error quaternion $\delta\boldsymbol{q}$. Moreover, in the nonadaptive ideal case, if the parameter $\boldsymbol{\theta}^*$ is exactly known (no uncertainty), then the filtered control signal specified in Eq. (19) can be replaced by simply using $\boldsymbol{u}_f = -W_f\boldsymbol{\theta}^*$, ultimately leading to

$$\boldsymbol{u} = \alpha\boldsymbol{u}_f + \dot{\boldsymbol{u}}_f = -W\boldsymbol{\theta}^*$$

thereby obviating any need for the regressor filter of Eq. (12) during controller implementation.

3) It is always possible to introduce the filter states such that $\boldsymbol{\eta}(t) = 0$ for all $t \geq 0$ by letting $\boldsymbol{\eta}(0) = 0$ based on the suitable selection of initial filter states such as

$$\boldsymbol{\omega}_f(0) = (\delta\boldsymbol{\omega}(0) + k_p\delta\boldsymbol{q_v}(0))/k_p$$

and $W_f(0) = 0$ in Eq. (20). This will further improve the transient performance of the closed-loop adaptive attitude control system, because $\boldsymbol{\eta}(t) = 0$ eliminates the time and control effort needed toward enabling the filter-state convergence. Of course, as seen from the preceding Proof, even in the case that $\boldsymbol{\eta}(0) \neq 0$, closed-loop stability and overall convergence of the trajectories to the attracting manifold $\mathcal{S}$ remains true, and the signal $\boldsymbol{\eta}(t)$ still converges to zero exponentially fast. However, having $\boldsymbol{\eta}(0) = 0$ permits us to rewrite the dynamics governing the parameter-estimation error signal $\boldsymbol{z}$ given in Eq. (21) as follows:

$$\dot{\boldsymbol{z}} = -\gamma W_f^T J^{-1} W_f \boldsymbol{z} \tag{27}$$

which is linear with respect to the parameter-estimation error $\boldsymbol{z}$. Thus, if the parameter-estimation error $\boldsymbol{z}$ is equal to zero at any instant of time t, then adaptation stops henceforth and parameter estimates thereby stay locked at their true values [i.e., if $\boldsymbol{z}(t^*) = 0$ for some $t^* > 0$, then $\boldsymbol{z}(t) = 0$ for all $t \geq t^*$]. We emphasize here that this nice feature is available only if the filter initial conditions are chosen such that $\boldsymbol{\eta}(0) = 0$, and such a possibility is never available with existing CE-based formulations.

4) Finally, one needs to be extra careful when interpreting the properties of the attracting-manifold definition $\mathcal{S}$ defined in Eq. (25) to the extent that $\lim_{t\to\infty}\boldsymbol{z}(t) = 0$ obviously implies $\lim_{t\to\infty}W_f(t)\boldsymbol{z}(t) = 0$, but the converse is not necessarily true. Therefore, just as with CE-based controllers, even under the proposed non-CE adaptive control scheme, there is no recourse from ensuring satisfaction of suitable PE conditions on the reference trajectory if one is interested in ensuring convergence of all the parameter estimates to their respective unknown true values.

IV. Numerical Simulations

To demonstrate the various features of the proposed adaptive attitude control method, we perform numerical simulations and compare the closed-loop trajectory-tracking simulation results with the quaternion CE-based adaptive control results from [7]. Two sets of simulations are performed. In the first case, the reference trajectory does not satisfy the underlying persistence of excitation conditions to ensure convergence of parameter estimates to their corresponding true unknown values. The second set of simulations consider a persistently exciting reference trajectory.

The numerical model for the attitude-tracking control system has the following system parameters. The unknown inertia matrix is described by

$$\boldsymbol{\theta}^* = [20, 1.2, 0.9, 17, 1.4, 15]^T$$

The corresponding CE-based adaptive control law taken from [7] is listed next:

$$\boldsymbol{u}_{\text{ce}} = 2(P^{-1})^T\left[-Y\hat{\boldsymbol{\theta}}_{\text{ce}} - K\boldsymbol{r} - \frac{\delta\boldsymbol{q_v}}{1 - \delta\boldsymbol{q}_{\boldsymbol{v}}^T\delta\boldsymbol{q_v}}\right]; \qquad \dot{\hat{\boldsymbol{\theta}}}_{\text{ce}} = \Gamma Y^T\boldsymbol{r} \tag{28}$$

where

$$\boldsymbol{r} \doteq \delta\boldsymbol{q_v} + \alpha_{\text{ce}}\delta\dot{\boldsymbol{q}}_{\boldsymbol{v}}$$

$$P \doteq \delta q_o I_{3\times 3} + S(\delta \boldsymbol{q}_v)$$

corresponds to the vector part operator of $E(\boldsymbol{q})$ in Eq. (2); $Y \in \mathbb{R}^{3\times 6}$ is a regressor matrix corresponding to W in Eq. (10); α_{ce} and $K \in \mathbb{R}^{3\times 3}$ are constant, positive-definite, diagonal gain matrices; and $\Gamma \in \mathbb{R}^{6\times 6}$ is any learning-rate matrix that is also constant, positive-definite, and diagonal. In the following simulations, the initial value of the parameter estimate for both $\boldsymbol{u}$ and $\boldsymbol{u}_{\mathrm{ce}}$ is chosen to be

$$\hat{\boldsymbol{\theta}}(0) + \boldsymbol{\beta}(0) = \hat{\boldsymbol{\theta}}_{\mathrm{ce}}(0) = [21, 2.2, 1.9, 18, 24, 16]^T$$

the initial body quaternion is

$$\boldsymbol{q}(0) = [\sqrt{1 - 3 \times 0.1826^2}, 0.1826, 0.1826, 0.1826]^T$$

and the reference quaternion is $\boldsymbol{q}_C(0) = [1, 0, 0, 0]^T$. The body is initially at rest and the corresponding reference angular-velocity profile is given at each simulation.

A. Non-PE Reference Trajectory

For the first set of simulations, we consider a non-PE reference trajectory described by

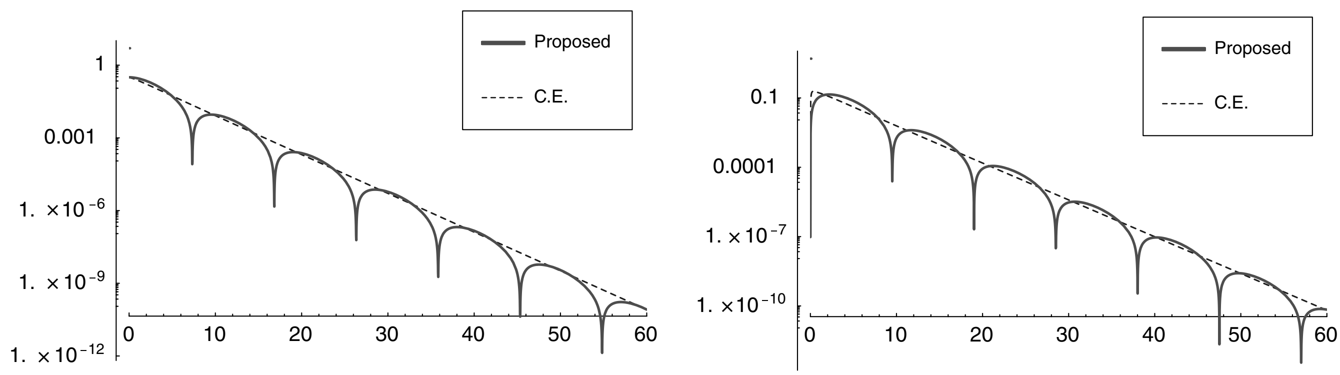

a) Quaternion tracking error $\delta \boldsymbol{q}_v$

b) Angular velocity error $\delta \boldsymbol{\omega}$

Fig. 1 Ideal-case closed-loop performance obtained with the CE-based and the proposed non-CE controller, assuming the inertia matrix J to be known.

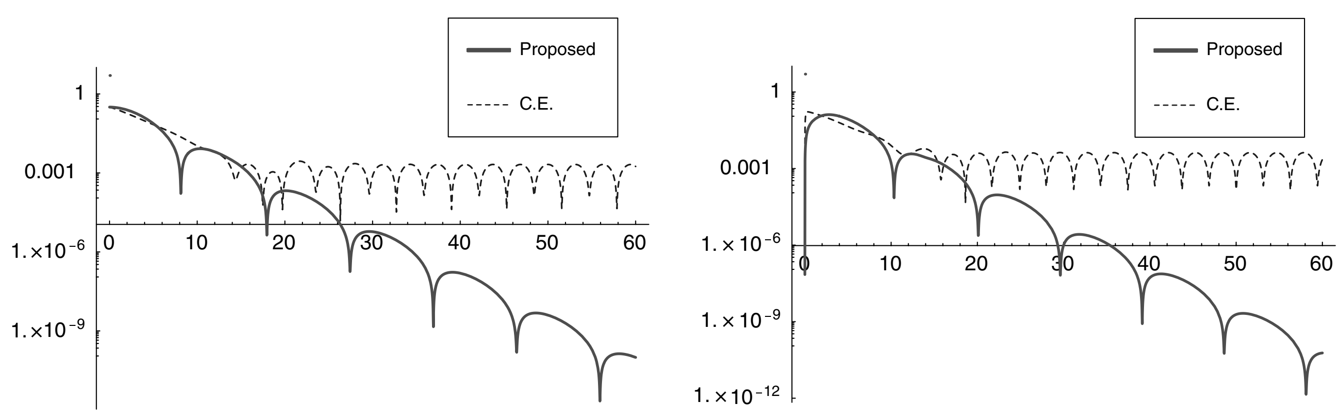

a) Quaternion error $\delta \boldsymbol{q}_v$

b) Angular velocity error δ_ω

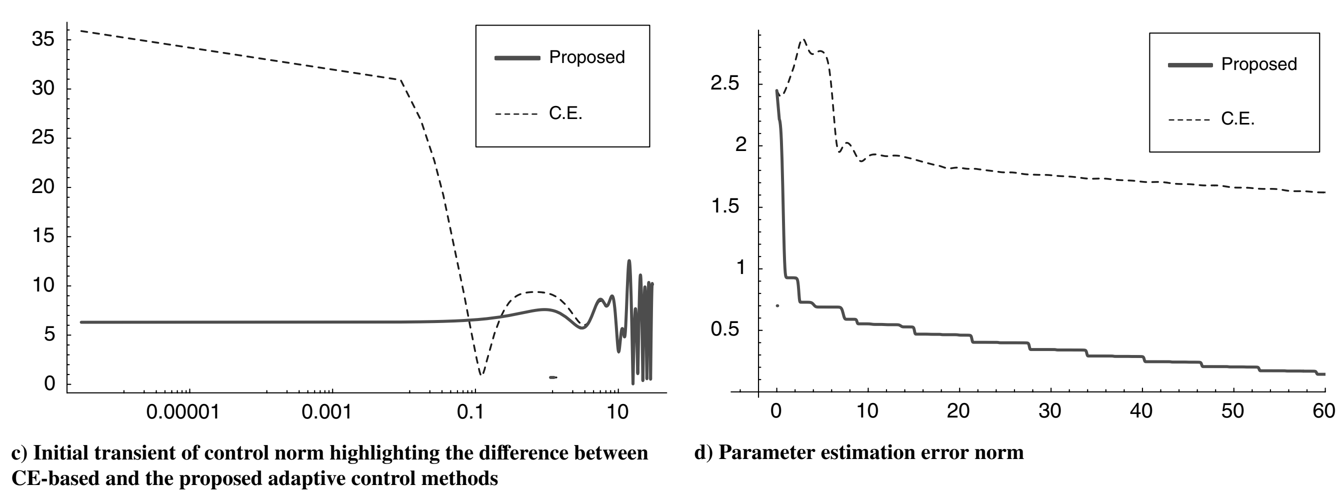

c) Initial transient of control norm highlighting the difference between CE-based and the proposed adaptive control methods

d) Parameter estimation error norm

Fig. 2 Adaptive attitude-tracking closed-loop-performance comparison between the classical CE-based controller and the proposed non-CE controller for a non-PE reference trajectory.

$$\omega_C(t) = [0.3(1 - e^{-0.01t^2}) \cos t + te^{-0.01t^2}(0.08\pi + 0.006 \sin t)] \cdot [1, 1, 1]^T \tag{29}$$

To permit a fair and meaningful comparison between the CE-based controller and proposed non-CE adaptive controller, we tuned the various controller parameters to obtain similar error convergence rates, as shown in Fig. 1, assuming that the inertia matrix J is known (ideal-case performance).

The corresponding control gains are determined as follows: $\alpha_{ce} = \text{diag}\{10, 10, 10\}$, $K = \text{diag}\{7.5, 7.5, 7.5\}$, every element of Γ is set as zero for the CE-based method; and $k_v = 0.5$, $k_p = 0.5$, and $\gamma = 0$ for the proposed method. The wriggle seen in Fig. 1 for the proposed method is from the fact that the deterministic/ideal-case error dynamics (described by Eq. (20) with $W_f z = 0$) correspond to a second-order system, whereas the ideal-case closed-loop dynamics under the CE-based method result in a stable first-order system in terms of the composite error signal $\boldsymbol{r}$ (for further details, refer to [7]).

Next, we assume the inertia matrix J to be unknown and simulate both the CE and non-CE adaptive controllers, which means that

$$\Gamma = \text{diag}\{0.1, 0.1, 0.1, 0.1, 0.1, 0.1\}$$

and $\gamma = 100$. The resulting closed-loop simulations are documented in Fig. 2. Initial filter-state values for the proposed method are chosen as follows: $W_f(0) = 0$ and

$$\boldsymbol{\omega}_f(0) = (\delta\boldsymbol{\omega}(0) + k_p \delta\boldsymbol{q_v}(0))/k_p$$

thereby satisfying $\boldsymbol{\eta}(t) = 0$ for all $t \geq 0$. The learning rate Γ of the CE-based adaptive control method in Eq. (1) and its counterpart γ for the proposed adaptive controller are systematically tuned to achieve performance that is as close as possible to the ideal-case performance obtained for both methods in Fig. 1. The attitude and angular-rate errors converge to zero with both adaptive controllers. As seen in Figs. 2a and 2b, the closed-loop performance from the proposed method with inertia uncertainty remains more or less the same when compared with the corresponding ideal-case performance in Fig. 1. This is clearly not the case with the CE-based controller, because the attitude and angular-rate errors exhibit a very slow convergence trend in Fig. 2. To see the asymptotic convergence of tracking errors with the CE-based results, a long simulation time is required. We note that one may find a different combination of CE-based control parameters that could deliver better performance, but the parameter set used for the CE-based controller used in our simulations is determined after exhaustive search to ensure best-possible performance. The norms of the control torques commanded by the CE-based controller and the non-CE controller are both plotted in Fig. 2c, in which it can be clearly seen that the torque demands due to the CE-based adaptive controller are severe during the initial transient. Given that we are simulating a trajectory-tracking problem, the steady-state torques obviously remain time-varying to ensure tracking along the prescribed reference trajectory. The parameter-estimation error norms are compared in Fig. 2d. We recognize that parameter-estimation error fails to converge to zero for both methods, due to the non-PE nature of the underlying reference trajectory.

The role played by the parameter γ in the proposed adaptive controller is studied next. It is clear from Eq. (21) that whenever $\boldsymbol{\eta}(0) = 0$, the attractiveness of manifold $\mathcal{S}$ can be accelerated by increasing the value of γ parameter. This implies that the ideal-case (no uncertainty) closed-loop performance can be closely recovered with increasing γ values. We consider two different γ values ($\gamma = 10$ and 100) and report the simulation results in Fig. 3. For the larger-γ case, the attitude-tracking performance is improved, as seen from the faster attitude and angular-rate error convergence in Figs. 3a and 3b. Parameter-estimation error with large γ also converges faster than the case with small γ in Fig. 3d, because the manifold attractivity of

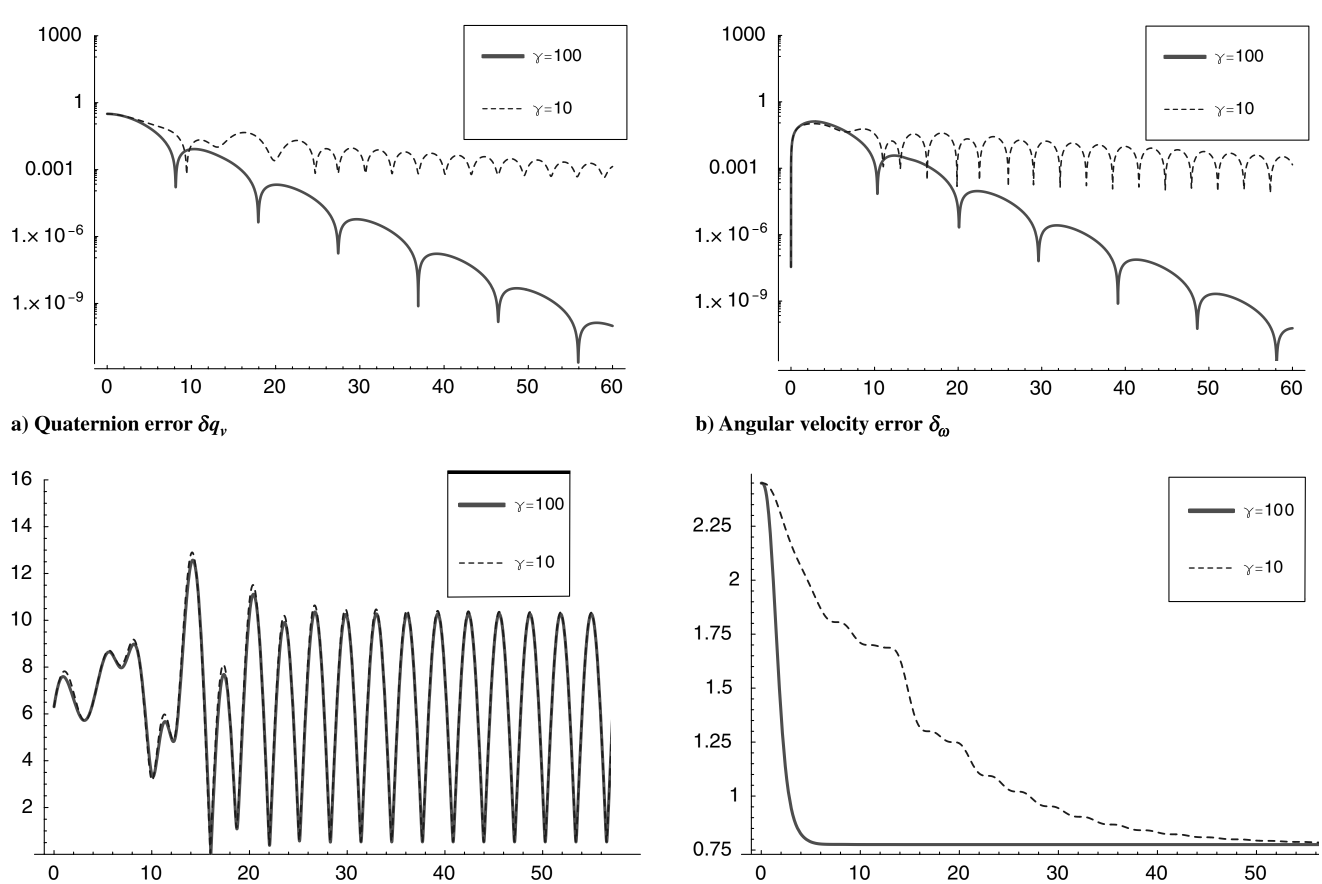

a) Quaternion error δq_v b) Angular velocity error δ_ω c) Control norm d) Parameter estimation error norm

Fig. 3 Performance study of the proposed non-CE adaptive attitude-tracking controller for two different γ values.

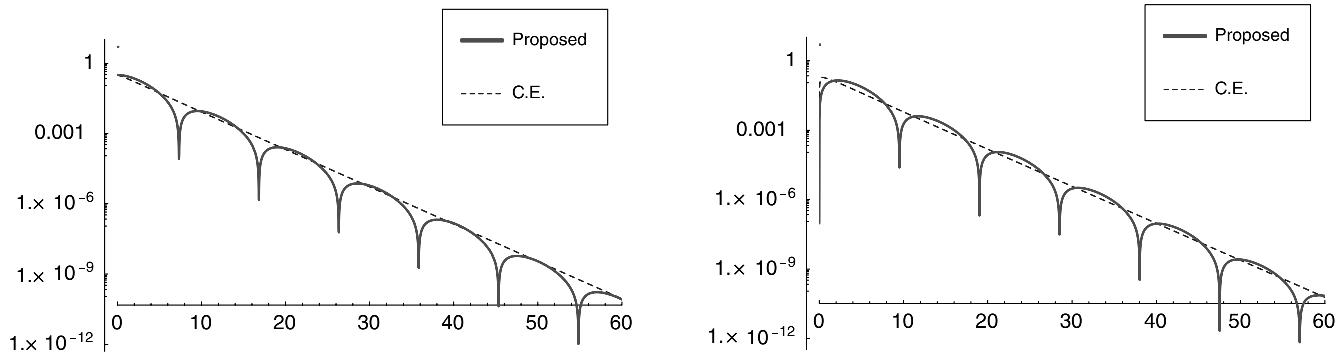

a) Quaternion error δq_v **b) Angular velocity error δ_ω**

Fig. 4 Ideal-case closed-loop performance for the PE reference trajectory obtained with the CE-based and the proposed non-CE controller, assuming the inertia matrix J to be known.

Eq. (27) is increased. In Fig. 3c, we recognize that the peak control norm is mostly unchanged, in spite of the increased γ value, because the reduction in the parameter-estimation error due to the larger γ value contributes to a decrease in the control norm during the transient part of the simulation.

B. PE Reference Trajectory

We now consider the case wherein the reference trajectory is persistently exciting so that parameter estimates from the CE-based controller and the proposed non-CE controller may converge to their corresponding true values. The reference angular velocity for this simulation is taken to be

$$\boldsymbol{\omega}_{\mathrm{CP}}(t) = [\cos t + 2, 5\cos t, \sin t + 2]^T$$

Before comparing the closed-loop performance of each method, we first tune the deterministic (ideal-case nonadaptive) control performance, as done in Fig. 4, which leads to $\alpha_{\mathrm{ce}} = 8$ (the rest of the control gains are the same as before). The inertia matrix is once again assumed unknown, and the adaptive control simulations for the PE reference trajectory case are shown in Fig. 5. First, we note that the attitude and angular-rate error convergence remains slow with the CE-based method. Because the reference trajectory is persistently exciting, the parameter estimates converge to their true values and this convergence rate is significantly faster for the proposed method than with the CE-based approach, as seen in Fig. 5d.

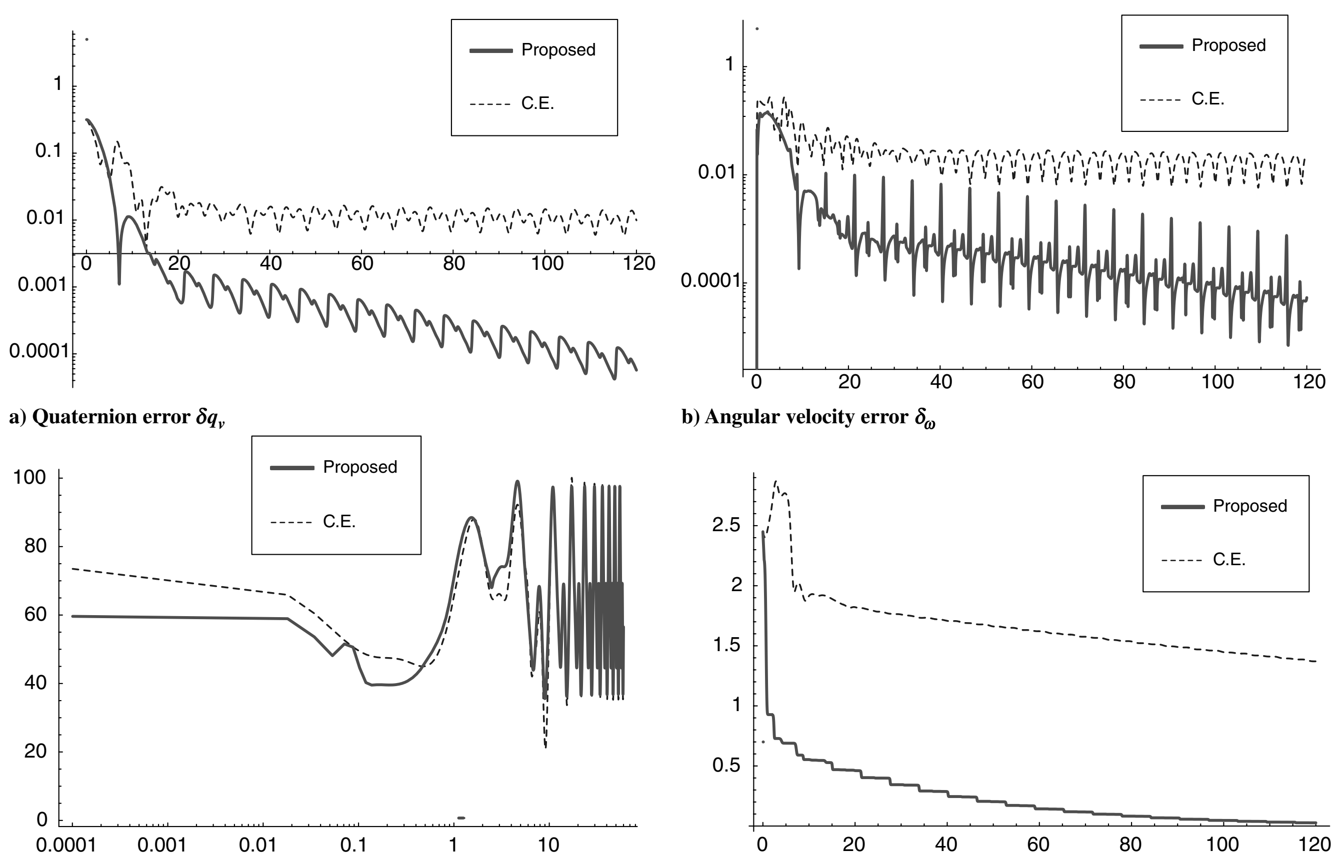

a) Quaternion error δq_v **b) Angular velocity error δ_ω**

c) Control norm **d) Parameter estimation error norm**

Fig. 5 Adaptive attitude-tracking closed-loop-performance comparison between the classical CE-based controller and the proposed non-CE controller for a PE reference trajectory.

V. Conclusions

A new noncertainty-equivalence adaptive control formulation for the attitude-tracking problem was formulated. The controller employs an attracting manifold that enables asymptotic recovery of closed-loop performance obtained under the ideal case (no uncertainty). The noncertainty-equivalence adaptive controller design is largely due to the innovative construction of the regressor filter. Global stability and asymptotic convergence of attitude and angular-velocity tracking errors are guaranteed for arbitrarily large uncertainties in the inertia matrix. In addition, we place no further restrictions on persistence of excitation due to the reference trajectory.

Acknowledgments

This work was supported in part by the National Science Foundation under grant CMS-0409283 and the NASA Goddard Space Flight Center under grant NNG04GB18G.

References

[1] Wen, J. T., and Kreutz-Delgado, K., "The Attitude Control Problem," *IEEE Transactions on Automatic Control*, Vol. 36, No. 10, 1991, pp. 1148–1162.
doi:10.1109/9.90228

[2] Bhat, S. P., and Bernstein, D. S., "A Topological Obstruction to Continuous Global Stabilization of Rotational Motion and the Unwinding Phenomenon," *Systems and Control Letters*, Vol. 39, No. 1, 2000, pp. 63–70.
doi:10.1016/S0167-6911(99)00090-0

[3] Schaub, H., and Junkins, J. L., *Analytical Mechanics of Space Systems*, AIAA Education Series, AIAA, Reston, VA, 2003, Chap. 3.

[4] Krstić, M., and Tsiotras, P., "Inverse Optimal Stabilization of a Rigid Spacecraft," *IEEE Transactions on Automatic Control*, Vol. 44, No. 5, 1999, pp. 1042–1049.
doi:10.1109/9.763225

[5] Junkins, J. L., Akella, M. R., and Robinett, R. D., "Nonlinear Adaptive Control of Spacecraft Maneuvers," *Journal of Guidance, Control, and Dynamics*, Vol. 20, No. 6, 1997, pp. 1104–1110.

[6] Schaub, H., Akella, M. R., and Junkins, J. L., "Adaptive Control of Nonlinear Attitude Motions Realizing Linear Closed-Loop Dynamics," *Journal of Guidance, Control, and Dynamics*, Vol. 24, No. 1, 2001, pp. 95–100.

[7] Costic, B. T., Dawson, D. M., de Queiroz, M. S., and Kapila, V., "Quaternion-Based Adaptive Attitude Tracking Controller Without Velocity Measurements," *Journal of Guidance, Control, and Dynamics*, Vol. 24, No. 6, 2001, pp. 1214–1222.

[8] Sastry, S., and Bodson, M., *Adaptive Control: Stability, Convergence, and Robustness*, Prentice–Hall, Upper Saddle River, NJ, 1989, Chap. 3.

[9] Ioannou, P., and Sun, J., *Robust Adaptive Control*, Prentice–Hall, Upper Saddle River, NJ, 1996, pp. 200–201.

[10] Astolfi, A., and Ortega, R., "Immersion and Invariance: A New Tool for Stabilization and Adaptive Control of Nonlinear systems," *IEEE Transactions on Automatic Control*, Vol. 48, No. 4, 2003, pp. 590–606.
doi:10.1109/TAC.2003.809820

[11] Ortega, R., Hsu, L., and Astolfi, A., "Immersion and Invariance Adaptive Control of Linear Multivariable Systems," *Systems and Control Letters*, Vol. 49, No. 1, 2003, pp. 37–47.
doi:10.1016/S0167-6911(02)00341-9

[12] Akella, M. R., "Adaptive Control—A Departure from the Certainty Equivalence Paradigm," *Journal of the Astronautical Sciences*, Vol. 52, Nos. 1–2, 2004, pp. 75–91.

[13] Tsiotras, P., "Further Passivity Results for the Attitude Control Problem," *IEEE Transactions on Automatic Control*, Vol. 43, No. 11, 1998, pp. 1597–1600.
doi:10.1109/9.728877

[14] Marandi, S. R., and Modi, V. J., "A Preferred Coordinate System and the Associated Orientation Representation in Attitude Dynamics," *Acta Astronautica*, Vol. 15, No. 11, 1987, pp. 833–843.
doi:10.1016/0094-5765(87)90038-5

[15] Shuster, M. D., "A Survey of Attitude Representations," *Journal of the Astronautical Sciences*, Vol. 41, No. 4, 1993, pp. 439–517.

[16] Schaub, H., and Junkins, J. L., "Stereographic Orientation Parameters for Attitude Dynamics: a Generalization of the Rodrigues Parameters," *Journal of the Astronautical Sciences*, Vol. 44, No. 1, 1996, pp. 1–19.